JOURNAL OF CATALYSIS **139**, 540–550 (1993)

Reducibility of Ni–Mo/Al_2O_3 Catalysts: A TPR Study

JOAQUÍN L. BRITO AND JORGE LAINE

Laboratorio de Fisicoquímica de Superficies, Centro de Química, Instituto Venezolano de Investigaciones Científicas, I.V.I.C., Apartado 21827, Caracas 1020-A, Venezuela

Received April 6, 1992; revised July 24, 1992

Temperature-programmed reduction (TPR) has been employed to study the reducibility of Ni–Mo/γ-Al_2O_3 catalysts (0–5 wt% NiO; 12 wt% MoO_3) calcined at temperatures (T_C) between 400 and 800°C. Catalysts were further characterized by XRD, BET area, and ammonia adsorption measurements. Ni/Al_2O_3 samples showed two broad TPR bands: Ni_I, at lower temperature (T_m), assigned to a surface phase with similar stoichiometry to $NiAl_2O_4$, and the high T_m Ni_{II}, assigned to bulk-like $NiAl_2O_4$. On increasing T_C, Ni_{II} area increases at the expense of Ni_I. Mo/Al_2O_3 catalysts showed spectra with two peaks which were almost insensitive to varying T_C up to 660°C. The low-T_m Mo_I peak was assigned to (partial) reduction of polymolybdates, and the high-T_m Mo_{II} to further reduction of polymolybdates plus that of more refractory tetrahedrally coordinated and/or monomeric species. In Ni–Mo catalysts, XRD and NH_3 adsorption measurements, together with TPR data, indicate surface interaction between Ni and Mo, probably through the formation of Ni–Mo–O surface phases precursors of β-$NiMoO_4$. Ni facilitated the reduction of Mo, as the T_m of the Mo_I peak decreased on increasing Ni content between 0 and 5 wt% NiO. This effect was less apparent upon increasing T_C, indicating that it is related to the presence of Ni in or near the surface. However, quantitative TPR suggested that no appreciable amount of Ni was reduced simultaneously with Mo_I, and that the extent of Mo_I reduction was not affected by varying Ni concentration. In a similar way, Mo facilitated reduction of Ni, as reflected in the lower T_m of the Ni_I band in presence of Mo. Thus synergistic effects between Ni and Mo may be opperative not only in the sulfided state but also in the oxidic precursor of the catalysts. It is speculated that Ni ions responsible for Ni_I might be involved in the generation of active Ni–Mo–S phases. © 1993 Academic Press, Inc.

INTRODUCTION

Nickel–molybdenum hydrodesulfurization (HDS) catalysts have received less attention than the cobalt-promoted formulation, and as result less information on the physicochemical characteristics of both their oxidic and sulfide states is presently available (*1–4*). Moreover, in many cases results obtained on Co–Mo catalysts have been generalized to the Ni–Mo system (*2*, *3*), and much of what is "known" of the latter has been inferred from the properties and characteristics of the more conventional Co–Mo/Al_2O_3 catalysts. However, due to increasing demands for treating feeds of low H/C ratio and high nitrogen content (*5*), it may become desirable in the near future to substitute (at least partially) Ni for Co in commercial formulations, because of the better hydrogenating, hydrocracking, and hydrodenitrogenation functions of the Ni–Mo pair (*2*, *6*). Therefore, more detailed research on the Ni-promoted system is clearly needed.

The active sites of these catalysts are generated by means of reductive pretreatments, specifically sulfiding in reductive atmospheres. Thus, reduction studies of molybdena-based catalysts have often been employed for characterization purposes. In particular, hydrogen reduction is one of the more simple chemical ways (as compared, e.g., with sulfiding or HDS activity) for the characterization of these solids and their reactivity. At least two groups have studied the reducibility of Ni–Mo/Al_2O_3 catalysts by means of series of gravimetric measurements under hydrogen atmospheres, either under temperature-programmed conditions

0021-9517/93 $5.00

(*7*) or isothermally (*8*). More recently, temperature-programmed reduction (TPR) involving continuous analysis of the reactant atmosphere has also been employed (*9*, *10*). Gravimetric measurements on Ni–Mo/Al_2O_3 gave an unclear picture, similar to that previously available for Co–Mo/Al_2O_3 catalysts (*1*); i.e., some authors reported that Ni enhanced (*7*), and others that it inhibited (*8*), the reducibility of Mo compounds. The TPR results cited above (*10*) have not clarified this state of affairs. This situation is, in part, due to the limited range of reduction temperatures employed in these studies (up to 600°C), which has prevented the examination of all the species present in the catalysts. However, Arnoldy *et al.* (*11*) have shown that in the case of Co–Mo catalysts TPR carried out up to, roughly, 1000°C may give a clearer picture of the structure and reducibility of the oxidic precursors than the conventional studies performed at lower reduction temperatures.

The aim of the present work is to study the complete reducibility of Ni and Mo species in Ni–Mo/Al_2O_3 catalysts using TPR. The effects of varying Ni concentration and calcination temperature in the reducibility of catalysts with Mo content typical of commercial hydrotreatments catalysts are investigated.

EXPERIMENTAL

Preparation of Catalysts

Catalysts were prepared by incipient wetness ("dry") impregnation of a commercial γ-Al_2O_3 (Filtrol, SV-1038 A, crushed and sieved to 60–150 mesh). Molybdenum was first added from an ammonium heptamolybdate solution, followed by drying (overnight at 120°C) and calcination (2 h at 400°C). Portions of this solid were then "dry" impregnated with nickel nitrate solutions in order to get solids with 1, 3, and 5 wt% NiO. After overnight drying, the different compositions were divided in several parts and submitted to the following procedure: All of them were calcined at 400°C overnight before removing one portion of each composition and increasing the temperature to 500°C. After 2 h another set of samples was removed, and this was repeated again after 2 h at 600, 660, and 800°C. The solids thus prepared included catalysts with only Mo (12 wt% as MoO_3) and only Ni (5 wt% as NiO), and will be identified with symbols such as $X/Y\,(T_C)$, where X and Y are the wt% of NiO and MoO_3, respectively, and T_C is the calcination temperature in °C.

Catalyst Characterization

BET surface areas were measured by means of a commercial sorptometer, modified in order to perform "*in situ*" pretreatments. *X-ray diffraction* (XRD) analysis of the catalyst samples was carried out with a Philips PW 1730 instrument, using Ni-filtered CuK_α radiation. The *acidity* of the surfaces, as given by the amount of ammonia adsorbed at 200°C and at an ammonia partial pressure of 300 Torr, was evaluated by a gravimetric technique described elsewhere (*12*).

Temperature-Programmed Reduction

The TPR apparatus has been described previously (*13*, *14*). The 100-mg samples of calcined catalyst, with no previous pretreatment, were introduced into the quartz reactor and rapidly heated under the reactant mixture (15 vol% H_2 in N_2, flowing at 40 ml/min) to the initial temperature (180°C). Afterwards, the run was started, heating at 20°C/min up to 930°C, and this temperature was held until stability of the TCD signal was attained. It was confirmed that no TPR peaks exist at less than 180°C for any of the solids studied.

TPR spectra were quantified by means of a "cut and weight" method, that allowed us to calculate H_2 consumption by measuring the area of peaks (after substracting the small contribution due to the support). In most cases it was possible to discriminate between well differentiated peaks. In several instances, however, peak superimposition prevented a clear differentiation of the signals, and peak deconvolution in good quality millimeter-quadrille paper was carried out. Standards employed to calibrate the TCD response included pure oxides such as MoO_3, NiO (*14*), CuO (*15*), etc. The accuracy of the measurements was cross-checked by comparing several TPR runs of samples of both standards and catalysts, and it was found to be better than 5% in the first case, and between 5 and 10% in the case of catalysts (assuming their nominal composition). Generally, the quantitative assessment of the composition of catalysts by TPR became poorer on increasing T_C, presumably due either to loss of volatile material or to formation of phases more refractory to reduction (see below).

RESULTS

Physicochemical Characteristics of the Catalysts

Table 1 shows the composition, color and surface area of the oxidic samples of the catalysts. Figure 1 presents selected XRD traces. The catalysts calcined at T_C up to 660°C show only the broad bands related to the γ-Al_2O_3 support, as exemplified by the diffractogram of sample 5/12 (660) (Fig. 1e). This suggests high dispersion of the Ni–Mo supported compounds. Samples calcined at 800°C show also signals due to the support, plus small peaks related to single or mixed oxides of Mo, Ni, and Al. In the case of samples with Mo and low or no Ni content, 1/12 (800) and 0/12 (800), almost all of these peaks agree with the signals of $Al_2(MoO_4)_3$ (JCPDS Powder Diffraction File card 23-764), as indicated by the keys in Figs. 1a and 1b. On the other hand, sample 5/12 (800) (Fig. 1c) does not show the XRD trace of $Al_2(MoO_4)_3$, its most salient feature being a single peak at $2\theta = 26.8°$, that indicates the presence of β-$NiMoO_4$ (*16*). Interestingly, for the lower Ni contents the position of some alumina signals in Mo-containing catalysts change upon calcination at 800°C: While 5/0 (800) and 5/12 (800) show the same bands as the original γ-Al_2O_3, though somewhat sharper, 0/12 (800) and 1/12 (800) show new bands which could be related to the transition $\gamma \rightarrow \delta$-$Al_2O_3$. This idea stems from the disappearance of the peak at about $2\theta = 37.5°$ (associated to γ-Al_2O_3) and the apparition of the one at $2\theta = 36.6°$ (due to δ-Al_2O_3). The increased crystallinity of either support phase (γ- or δ-Al_2O_3) is in line with the decreased BET area (Table 1).

Ammonia adsorption data is displayed in Fig. 2. Although differences are not too large between some of the samples, these results are highly reproducible, at least an order of magnitude better than, e.g., Hammet indicator-titration with amines (*12*). The incorporation of Ni alone to the support hardly affects the amount of NH_3 adsorbed on the surface, while the presence of MoO_3 results in a remarkable increase of the amount adsorbed. This effect has been previously reported (*12*) and explained on the basis of the higher acidity of Mo^{6+} oxides as compared to the alumina support, because Mo oxides stay "on top" of the catalyst surface. Variations induced by Ni in Ni–Mo catalysts calcined at a given temperature are smaller, showing maxima of NH_3 adsorption at 1 or 3 wt% NiO, depending on calcination temperature. Similar results in a different set of Ni–Mo catalyst calcined at 400°C have been presented and discussed elsewhere (*17*) and other workers have also reported similar data (*18*). The behavior of the series calcined at 500, 600, and 660°C have not been previously reported.

Temperature-Programmed Reduction

Figures 3 and 4 show the TPR spectra of the catalysts. Spectra taken at other heating rates (e.g., 5 or 10°C/min) showed similar features, although the temperatures at the maxima of the peaks (T_m) were displaced to lower values. Several TPR peaks may be observed, which will be referred to as: Mo_I (T_m between 455 and 500°C) and Mo_{II} (780–860°C), in Mo-containing catalysts; Ni_I (600–700°C) and Ni_{II} (800–850°C) in Ni-containing samples. Note that, in promoted catalysts, Mo_{II} and Ni_{II} peaks are completely superimposed and the high-tempera-

TABLE 1

Physicochemical Characteristics of Catalysts

Catalyst composition (wt% NiO/wt% MoO_3)	Calcination temperature (°C)	Surface area ($m^2 g^{-1}$)	Color
0/12	400	230	White
1/12	400	235	Light green
3/12	400	220	Light green
5/12	400	225	Light green
5/0	400	218	Grayish green
0/12	500	230	White
1/12	500	235	Light green
3/12	500	223	Light green
5/12	500	225	Light green
5/0	500	218	Grayish blue
0/12	600	233	White
1/12	600	223	Light green
3/12	600	210	Light blue
5/12	600	210	Light blue
5/0	600	198	Light blue
0/12	660	170	White
1/12	660	185	Light green
3/12	660	180	Light blue
5/12	660	175	Light blue
5/0	660	203	Light blue
0/12	800	45	White
1/12	800	50	Light green
3/12	800	48	Light blue
5/12	800	50	Light blue
5/0	800	180	Light blue

ture tail of Ni_I overlaps the leading edge of Mo_{II}. Figures 5 and 6 show the T_m values of the different TPR peaks, as a function of calcination temperature and Ni content, respectively, while Table 2 shows quantitative data calculated from the TPR spectra.

The TPR traces of Ni/Al_2O_3 (a-spectra in Figs. 3 and 4) are characterized by the broad Ni_I and Ni_{II} bands, partially overlapping at the lower calcination temperatures. Upon increasing T_C Ni_I "migrates" to the region of Ni_{II}. It seems reasonable that the phase responsible for Ni_I is being transformed to the high-T_m one. For comparison, the TPR spectrum of the support is shown in Fig. 3A(f).

TPR spectra of Mo/Al_2O_3 samples are almost invariable with increasing T_C up to 600°C (Fig. 3, b-traces), and show a clear separation of the reduction process in two steps associated with the Mo_I and Mo_{II} peaks. Incorporation of Ni to the Mo-containing catalysts does not greatly affect the shape of the TPR patterns. However, at the lower calcination temperatures (400 and 500°C, Figs. 3A and 3B) an additional broad band in the region of Ni_I is present. Quantitative data (Table 2) shows that the area of Mo_I is quite independent of Ni content, and that, for samples calcined below 600°C, essentially all the nickel present is reduced under the Ni_I band. As in the case of Ni/

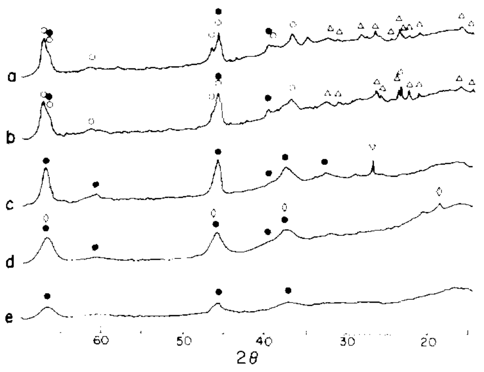

FIG. 1. XRD traces of selected catalyst samples: (a) 0/12 (800), (b) 1/12 (800), (c) 5/12 (800), (d) 5/0 (800), (e) 5/12 (660). Keys: ●, γ-Al_2O_3; ○ δ-Al_2O_3; △, $Al_2(MoO_4)_3$; ▽, β-$NiMoO_4$; ◇, Ni spinel ($2\ NiO \cdot 9\ Al_2O_3$).

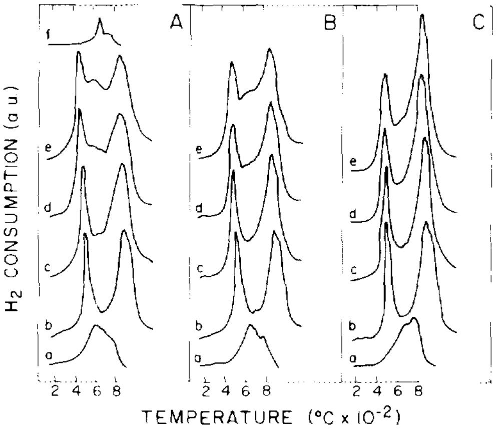

FIG. 3. TPR spectra of catalysts calcined at: (A) 400°C; (B) 500°C, and (C) 600°C. Catalyst composition (as wt% NiO/wt% MoO_3): (a) 5/0, (b) 0/12, (c) 1/12, (d) 3/12, (e) 5/12, and (f) γ-Al_2O_3 support.

Al_2O_3, Ni_I moves to higher temperatures upon increasing T_C and eventually (T_C 600°C or higher) it merges with the $Mo_{II}(+Ni_{II})$ peak, as demonstrated by the increasing size of the latter with increasing Ni content (Table 2).

DISCUSSION

Surface Interaction between Ni and Mo

Acidity data (Fig. 2) shows relatively strong increases in NH_3 adsorption associated to increasing T_C, that may be attributed to varying interaction between the support and Mo species. More subtle variations within series calcined at given temperatures suggest that Ni—which does not influence adsorption on the support—is able to modify the acidity of Mo compounds. It is concluded that surface interaction between Ni and Mo exists in catalysts calcined at less than 800°C. Chemical interaction between

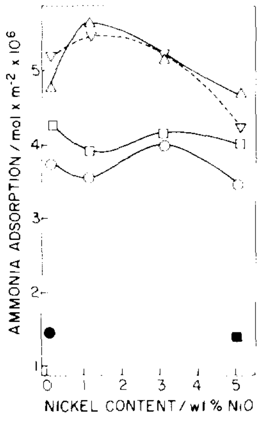

FIG. 2. Gravimetric measurements of ammonia adsorption on catalyst samples. Experimental conditions: 200°C, 300 Torr of NH_3. Keys: ●, support, calcined at 400°C; ■, 5/0 (400); ○, catalyst samples calcined at 400°C; □, at 500°C; △, at 600°C; ▽, at 660°C.

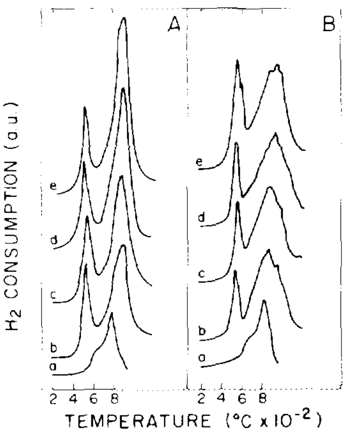

FIG. 4. TPR spectra of catalysts calcined at: (A) 660°C and (B) 800°C. Catalyst composition (as wt% NiO/wt% MoO_3): (a) 5/0, (b) 0/12, (c) 1/12, (d) 3/12, and (e) 5/12.

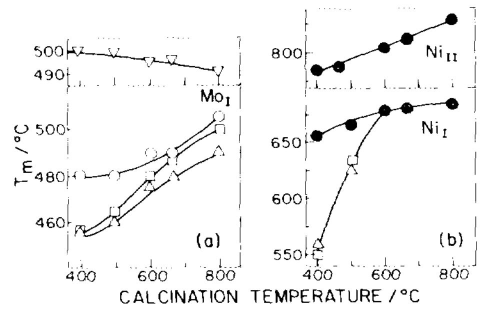

FIG. 5. Effect of calcination temperature on the T_m values of (a) Mo_I and (b) Ni_I and Ni_{II}. Keys: ▽, 0/12; □, 3/12; ○, 5/12; and ●, 5/0.

Ni and Mo in the oxidic form of Ni–Mo/Al_2O_3 has been proposed in the past on the basis of XPS (*19*) and ISS results (*20*, *21*). These results suggested that Ni would be located within the surface molybdate layer, but no evidence was found of a bilayer structure (i.e., Ni between Mo phases and the support), as proposed in the case of Co–Mo catalysts (*22*).

β-$NiMoO_4$ was detected at a T_C of 800°C, thus it may be assumed that the Ni–Mo mixed phases eventually evolve to this compound. In this regard it can be said that, from laser Raman measurements, Dufresne *et al.* (*19*) reported the presence of what they described as poorly crystalline β-$NiMoO_4$ in catalysts calcined at temperatures as low as 500°C. It must be pointed out that bulk β-$NiMoO_4$ is unstable at room temperature (*16*), which suggests a role of the support in its stabilization. On the other hand, the association of Ni with Mo is in line with the decreased formation of δ-Al_2O_3, reinforcing the view that Ni may help to prevent sintering of the support promoted by Mo phases (*23*).

Reducibility of Ni/Al_2O_3 Catalysts

The observation of two broad superimposed peaks in Ni catalysts calcined at the lower temperatures (Fig. 3, a-traces) agrees with a previous report by Houalla (*24*), and may be assigned to the presence of two distinct NiO–Al_2O_3 interaction compounds. The higher T_m one is similar to bulk $NiAl_2O_4$ in both color (readily observed in the high-T_C samples) and T_m (930°C or higher in similar conditions). The phase with lower T_m is different from NiO, which shows a sharp peak at about 400°C in the same experimental conditions (*14*). This phase could be related to a surface compound with the same stoichiometry than $NiAl_2O_4$, but with a different distribution of the Ni cations between sites with tetrahedral and octahedral symmetry. Scheffer *et al.* (*25*) have reported that the low-T_m phase corresponds to a surface interaction compound where Ni cations are all octahedrally coordinated. Dufresne *et al.* (*19*) also reported two different NiO–Al_2O_3 phases, depending on the calcination temperature of the catalyst. The more easily reducible phase was described as "bidimensional" $NiAl_2O_4$, while the other one was identified with bulk-like $NiAl_2O_4$.

Reducibility of Mo/Al_2O_3 Catalysts

Generally, the Mo_I peak of Mo/Al_2O_3 catalysts has been assigned to *partial* reduction of very dispersed polymolybdate-like species, while the Mo_{II} signal is thought to be the composite of the subsequent reduction of such species plus the reduction of more refractory entities, including tetrahedrally coordinated molybdate groups (*11*, *13*). Figure 5 shows that Mo_I is scarcelly affected

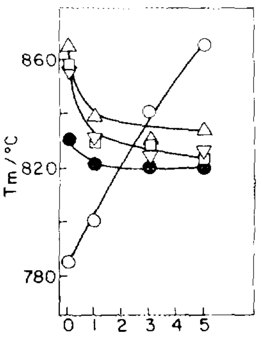

FIG. 6. Effect of Ni content on the T_m values of Mo_{II}(+Ni_{II}) peaks. Keys: △, calcined at 400°C; □, 500°C; ▽, 600°C; ●, 660°C; and ○, 800°C.

TABLE 2

Quantitative TPR Data of (Ni–)Mo/Al_2O_3 Catalysts

Catalyst	Area of TPR peaks (mmole H_2 g^{-1} catalyst)			
	1st peak[a]	2nd peak[b]	3rd peak[c]	Total
0/12 (400)	0.958	—	1.54	2.50
1/12 (400)	0.998	0.200	1.60	2.79
3/12 (400)	0.931	0.572	1.42	2.93
5/12 (400)	0.931	0.851	1.44	3.22
0/12 (500)	0.918	—	1.56	2.48
1/12 (500)	0.918	0.106	1.65	2.67
3/12 (500)	0.825	0.599	1.48	2.90
5/12 (500)	0.905	0.718	1.54	3.17
0/12 (600)	0.918	—	1.50	2.42
1/12 (600)	0.865	—	1.72	2.58
3/12 (600)	0.931	0.160	1.89	2.98
5/12 (600)	0.891	0.266	1.94	3.10
0/12 (660)	0.865	—	1.52	2.38
1/12 (660)	0.878	—	1.66	2.54
3/12 (660)	0.865	—	1.86	2.73
5/12 (660)	0.905	—	2.09	2.99
0/12 (800)	0.545	—	1.61	2.16
1/12 (800)	0.585	—	1.74	2.33
3/12 (800)	0.732	—	1.90	2.63
5/12 (800)	0.851	—	2.06	2.91

[a] Mo_I: T_m between 400 and 500°C.

[b] Ni_I: T_m around 600°C.

[c] $Mo_{II}(+Ni_{II})$: T_m higher than 740°C.

by varying T_C; Mo_{II} is more affected by the thermal history, its T_m decreasing with increasing T_C (Fig. 6). These observations agree with the proposed nature of the Mo species: Polymolybdates, although in close registry ("epitaxial") to the support, do not interact with it as strongly as the more refractory species, which should be more sensitive to changes induced by higher T_C's. It has been proposed that polarization effects of Al^{3+} ions may affect the covalency of the Mo–O bonds, and thus their reactivity toward hydrogen (*26*). Accordingly, the less polarized bonds of polymolybdates are easier to be reduced than those of the species directly tied to the supporting γ-Al_2O_3.

From Table 2 it can be seen that, in agreement with earlier literature (*1*) and with more recently published data (*27*, *28*), the average oxidation number of Mo after the first TPR peak (reduction up to ~600°C) is below 4 (about 3.7 for catalysts calcined at 660°C or less). This shows that reduction of supported polymolybdates proceeds, in part, to low oxidation states of Mo (Mo^{3+}, Mo^{2+}), even at mild reduction temperatures. After calcination at the higher T_C's (660 and 800°C) Mo_I becomes progressively smaller (Fig. 4, b-spectra) and the total H_2 consumption decreases by 4.8 and 13.6 vol%, respectively (Table 2). Arnoldy *et al.* (*11*) reported similar results when studying the Co–Mo/Al_2O_3 system, but they found more significant loss of reducible material when using a slightly higher T_C (850°C), and longer calcination times. Contrary to the present results, their most affected signal was the Mo_{II} peak. Decreased H_2 consumption suggests loss of Mo during calcination, probably by sublimation either as MoO_3 or as $MoO(OH)_2$. Sublimation of the latter should involve loss of surface OH groups, and this may account for the role of Mo in promoting accelerated sintering of the support (see, e.g., (*23*)) and the above reported transformation of γ- to δ-Al_2O_3. The preferential loss of polymolybdates (Mo_I peak) is parallelled by the formation of microcrystalline $Al_2(MoO_4)_3$ (Fig. 1a), whose TPR spectrum presents a single peak with T_m in the region of Mo_{II} (*29*).

Effect of Ni in Mo/Al_2O_3 Reducibility

This is the first systematic study, using TPR, of the complete reduction of Ni–Mo phases supported on alumina. In a previously published paper, Burch and Collins reported TPR patterns of several Ni–Mo/γ-Al_2O_3 catalysts (*10*), but they performed the TPR runs up to about 600°C, which limited the species studied and obscured the interpretation of the data, as shown below.

In an early report, Nag *et al.* (*9*) assigned the first TPR peak in Ni–Mo (and Co–Mo and Ni–W) supported catalysts to the Ni (Co) promotor. Burch and Collins (*10*) also proposed that, in Ni–Mo/Al_2O_3 industrial-type catalysts, most of the Ni reduces simultaneously with Mo under the low-T_m peak; however, they state that a substantial proportion of the Ni does not reduce until the temperature exceeds 800 K. Our quantitative data suggests that Ni^{2+} is not being reduced to any appreciable extent simultaneously with polymolybdates (Mo_I). We feel that the interpretation of Burch and Collins is affected by overlap of the Mo_I and Ni_I peaks, as they quantify as a whole not only the H_2 consumed under Mo_I, but also the amount consumed after isothermal heating for 1 h at 600°C. Although they do not explicitly report the sizes of their main peak for the different samples, they state that the area under this peak corresponds to an average change of 1 in the oxidation number of Mo, implying that this is true for all the Mo-containing samples, and thus that the area of this peak is independent of Ni content. Indeed, visual inspection of their spectra suggests that there are no significant differences in the sizes of the first peaks between unpromoted and promoted samples, although the shapes of the peaks are influenced by Ni content.

Nickel in the surface should be interacting with Mo (as suggested by NH_3 adsorption, Fig. 2) presumably as an "Ni–Mo–O"-type interaction phase. Either the amount of Ni involved in this phase is very small, as the differences in the sizes of Mo_I are negligible, or Ni is not reducible in the temperature range of Mo_I, probably because it is still associated to the support and, thus, stabilized after breakdown of the Ni–Mo–O phase due to reduction of Mo. However, the trends shown in Fig. 5 demonstrate that Ni influences the reducibility of Mo: Increasing T_C, which disfavors the presence of Ni^{2+} cations in or near the surface (*19, 21*) results in higher T_m's, while increasing Ni concentration is accompanied by decreased T_m's. This interpretation is in very good agreement with the results of Abart *et al.* (*7*). These authors found lower temperature onset of the weight loss due to reduction (T_R) upon increasing Ni content in the "molybdate layer" of Ni–Mo catalysts with the same overall composition (3 wt% NiO and 12 wt% MoO_3) but with reverse order of impregnation of Ni and Mo compounds. When Ni was impregnated "on top" of the molybdena catalyst, T_R was lower than when it was impregnated before Mo; the unpromoted catalyst presented the highest T_R value. The observed effect of Ni on the reducibility of polymolybdates establishes a difference with cobalt promoted catalysts, where variations in promoter content caused almost no effect on the T_m of the Mo_I peak (*11*). A possible role of Ni in enhancing

Mo reducibility could be to facilitate hydrogen activation (i.e., decomposition of H_2 to atomic hydrogen and migration to polymolybdates, e.g. by spill-over). This proposed activation of hydrogen by Ni has been invoked to explain the observed inhibition of coke formation on Mo catalysts promoted with Ni (*30*), and would account, in part, for the differences with the Co–Mo system, as Co is less efficient in H_2 activation.

Comparing the present data with TPR of NiO (single peak at 425°C), $NiMoO_4$ (main peak at 475°C) (*14*), $NiAl_2O_4$ (broad band around 930°C), and Ni/Al_2O_3 (Fig. 3 and 4, a-spectra), it is concluded that the Ni_I peak in $Ni–Mo/Al_2O_3$ corresponds to the low-T_m surface phase which is also present in Ni/Al_2O_3 catalysts. Note, however, that the T_m of the Ni_I band of catalysts calcined at 400 and 500°C are higher in the latter than in catalysts with Mo (Fig. 5b). Thus, and similarly to the case of Co–Mo supported catalysts (*11*), the presence of Mo seems to increase the reducibility of the low-T_m $NiO–Al_2O_3$ phase. This suggests that synergistic effects between Ni and Mo, which generally are thought to be opperative only in the sulfided state (*1–4*), could also be important in the oxidic precursors of the catalysts.

When Ni is present in Mo/Al_2O_3 catalysts, the losses of reducible material after calcination at the higher T_C's are smaller, suggesting that Ni prevents the sublimation of Mo oxides. Figure 6 shows that on increasing Ni content the T_m of the $Mo_{II}(+Ni_{II})$ peak decreases slightly, except for the samples calcined at 800°C, where the T_m increases strongly with Ni content. A similar behavior was also observed in the Co–Mo system (*11*), and it probably reflects structural changes in the highest T_C catalysts. Although XRD could not detect unequivocally Ni–Mo mixed oxides, except in the 5/12(800) sample, Mo fixation and decreased formation of $Al_2(MoO_4)_3$ suggest that Ni–Mo interaction does exist in the $Ni–Mo/Al_2O_3$ catalysts. As previously shown (*14*), $NiMoO_4$ presents a TPR spectrum with two peaks, the low-T_m one (around 500°C) being the most intense. Thus, also in this unsupported system the interaction with Ni renders Mo oxides more easily reducible, e.g., metallic Mo is readily formed at temperatures as low as 500°C (*14*).

Some attention has to be given to the strikingly different results reported by Fierro *et al.* (*8*), suggesting that the addition of Ni decreases the reducibility of Ni–Mo catalysts, in contradiction with our data and with that of Abart *et al.* (*7*). Burch and Collins state that their results are in broad agreement with Fierro's, although this is true only for their *estimation* of the extent of molybdenum reduction (*10*): While Fierro's group report decreased overall reduction of the catalysts induced by Ni, Burch and Collins show that the *total* reduction extent is higher upon increasing Ni content. The behavior observed by Fierro *et al.* may be explained by their peculiar pretreatment conditions, heating under vacuum at the desired reduction temperature until constant weight, before starting reduction in H_2 (the samples in the other three works were either not pretreated or preoxidized *in situ*). It is known that molybdena-based catalysts may undergo reduction by heating under vacuum (*31*). The ESR results of Fierro *et al.* show, indeed, reduction induced by heating *in vacuo* at the same temperatures employed thereafter for H_2 reduction measurements (*8*). Although the ESR data shows decreased Mo^{5+} signal with increasing Ni content, it must be remarked that only a fraction of the total Mo^{5+} formed (and no Mo^{4+}, if it is present) could be detected by this technique at room temperature (*32*). Thus, in the absence of a better explanation, we believe that the reported decreased reducibility of the catalysts by Ni is an artifact induced by the chosen pretreatment conditions.

Implications for the HDS Activity of Ni–Mo/Al$_2$O$_3$ Catalysts

Several workers have tried to correlate the reducibility of oxidic NiMo catalysts to the HDS activity of their sulfided state, with mixed results (see, e.g., (*10*)). This may be assigned to the fact that in Mo supported catalysts and under normal sulfiding conditions, O–S exchange is a more important reaction than reduction with H_2 (*33*). Thus, it is not generally true that phases more easily reducible are more sulfidable and/or active after sulfiding.

Ni–Mo/Al_2O_3 catalysts, on the other hand, have shown to be quite fragile to overheating during calcination (or oxidative regeneration), more so than the Co–Mo formulation. The optimum temperature for calcination of the oxidic precursors is held to be about 500°C (*10, 34*), catalysts fired at higher temperatures being poorer precursors for HDS catalysts. The most conspicuous change in our Ni–Mo catalysts upon increasing T_C is the disappearance of the Ni_I peak, and this occurs at T_C's higher than 500°C. Therefore, we tentatively propose that the Ni ions responsible for Ni_I in the promoted catalysts are involved in the generation of HDS-active Ni–Mo–S structures. These ions are most probably forming part of the Ni–Mo–O phase in fresh catalysts, as their depletion from the surface upon increasing T_C is accompanied by an increase of the T_m of Mo_I to the value observed in the unpromoted samples. Thus, it can be speculated that the Ni–Mo–S active phases are generated by sulfidation of already existing Ni–Mo–O interaction compounds.

CONCLUSIONS

The present results demonstrate that TPR can give a better insight of the reducibility of Ni–Mo/Al_2O_3 catalysts than the more conventional approaches employing limited temperature ranges and/or isothermal gravimetric measurements.

Acidity data indicates interaction between Ni and Mo in the oxidic state of the catalysts, probably as Ni–Mo–O surface phases. The XRD study shows that such phases eventually evolve to form crystalline β-$NiMoO_4$ at the highest calcination temperature. Quantitative TPR demonstrates (at least for the case of catalysts calcined at 400 and 500°C) that Mo and Ni phases reduce independently of each other. However, it also shows that the reduction of either one is facilitated by the presence of the other. Therefore, it is suggested that synergistic effects between Ni and Mo could be operative in the oxidic state of the catalysts.

Similarities exist with the Co–Mo/Al_2O_3 system, where also the reduction of promotor and Mo compounds occur independently and Co reduction is facilitated by the presence of Mo. As a variance, however, Co has no influence on the reducibility of Mo, while Ni is able to decrease the temperature of reduction of supported polymolybdates.

ACKNOWLEDGMENTS

This work was supported by the Consejo Nacional de Investigaciones Científicas y Tecnológicas (CONICIT). Thanks are due to Oswaldo Carías for the XRD measurements.

REFERENCES

1. Massoth, F. E., "Advances in Catalysis" (D. D. Eley, H. Pines, and P. B. Weisz, Eds.), Vol. 27, p. 265. Academic Press, New York, 1978.
2. Grange, P., *Catal. Rev.-Sci. Eng.* **21,** 135 (1980).
3. Topsøe, H., Clausen, B. S., Topsøe, N.-Y., and Pedersen, E., *Ind. Eng. Chem. Fundam.* **25,** 25 (1986).
4. Prins, R., de Beer, V. H. J., and Somorjai, G. A., *Catal. Rev.-Sci. Eng.* **31,** 1 (1989).
5. Speight, J. G., "The Desulfurization of Heavy Oils and Residua." Dekker, New York, 1981.
6. Laine, J., Severino, F., and Golding, R., *J. Chem. Technol. Biotechnol. A* **34,** 387 (1984).
7. Abart, J., Delgado, E., Ertl, G., Jeziorowski, H., Knözinger, H., Thiele, N., Wang, X.Zh., and Taglauer, E., *Appl. Catal.* **2,** 155 (1982).
8. Garcia-Fierro, J. L., Soria, J., and López-Agudo, A., *Appl. Catal.* **3,** 117 (1983).
9. Nag, N. K., Fraenkel, D., Moulijn, J. A., and Gates, G. C., *J. Catal.* **66,** 162 (1980).
10. Burch, R., and Collins, A., *Appl. Catal.* **18,** 389 (1985).
11. Arnoldy, P., Franken, M. C., Scheffer, B., and Moulijn, J. A., *J. Catal.* **96,** 381 (1985).
12. Laine, J., Yunes, S., Brito, J., and Andreu, P., *J. Catal.* **62,** 157 (1980).
13. Brito, J., and Laine, J., *Polyhedron* **5,** 179 (1986).
14. Brito, J. L., Laine, J., and Pratt, K. C., *J. Mater. Sci.* **24,** 425 (1989).
15. Laine, J., Brito, J., Severino, F., Castro, G., Tacconi, P., Yunes, S., and Cruz, J., *Catal. Lett.* **5,** 45 (1990).

16. Brito, J. L., and Laine, J., *Appl. Catal.* **72,** L13 (1991).
17. Laine, J., Brito, J., and Yunes, S., *in* "Proceedings of the Third International Conference on the Chemistry and Uses of Molybdenum" (H. F. Barry and P. C. H. Mitchell, Eds.), p. 111. Climax Molybdenum Co., Ann Arbor, Michigan, 1979.
18. Iannibello, A., Marengo, S., and Villa, P. L., *in* "Proceedings of the Third International Conference on the Chemistry and Uses of Molybdenum" (H. F. Barry and P. C. H. Mitchell, Eds.), p. 92. Climax Molybdenum Co., Ann Arbor, Michigan, 1979.
19. Dufresne, P., Payen, E., Grimblot, J., and Bonnelle, J. P., *J. Phys. Chem.* **85,** 2344 (1981).
20. Jeziorowski, H., Knözinger, H., Taglauer, E., and Vogdt, C., *J. Catal.* **80,** 286 (1983).
21. Kasztelan, S., Grimblot, J., and Bonnelle, J. P., *J. Phys. Chem.* **91,** 1503 (1987).
22. Delannay, F., Haeussler, E., and Delmon, B., *J. Catal.* **66,** 469 (1980).
23. Laine, J., and Pratt, K. C., *Ind. Eng. Chem. Fundam.* **20,** 1 (1981).
24. Houalla, M., *in* "Preparation of Catalysts III" (G. Poncelet, P. Grange, and P. A. Jacobs, Eds.), Stud. Surf. Sci. and Catal., Vol. 16, p. 273. Elsevier, Amsterdam, 1983.
25. Scheffer, B., Molhoek, P., and Moulijn, J. A., *Appl. Catal.* **46,** 11 (1989).
26. Arnoldy, P., and Moulijn, J. A., *J. Catal.* **93,** 38 (1985).
27. Redey, A., Goldwasser, J., and Hall, W. K., *J. Catal.* **113,** 82 (1988).
28. Yamada, M., Yasumaru, J., Houalla, M., and Hercules, D. M., *J. Phys. Chem.* **95,** 7037 (1991).
29. López-Cordero, R., López-Guerra, S., Fierro, J. L. G., and López-Agudo, A., *J. Catal.* **126,** 8 (1990).
30. Laine, J., Brito, J., Severino, F., *Appl. Catal.* **15,** 333 (1985).
31. Seshadri, K. S., and Petrakis, L., *J. Catal.* **30,** 195 (1973).
32. Seshadri, K. S., and Petrakis, L., *J. Phys. Chem.* **74,** 4102 (1970).
33. Arnoldy, P., van den Heijkant, J. A. M., de Bok, G. D., and Moulijn, J. A., *J. Catal.* **92,** 35 (1985).
34. Laine, J., Pratt, K. C., and Trimm, D. L., *J. Chem. Technol. Biotechnol.* **29,** 397 (1979).